

Hyphenated thermal analysis for in situ study of $(\text{Bi,Nd})_4\text{Ti}_3\text{O}_{12}$ formation from aqueous solution–gel synthesis

A. Hardy · H. Van den Rul · M. K. Van Bael · J. Mullens

Received: 11 December 2008 / Accepted: 12 February 2009 / Published online: 19 June 2009
© Akadémiai Kiadó, Budapest, Hungary 2009

Abstract High-temperature X-ray diffraction, absorption–reflection infrared spectrometry and thermal analysis coupled on-line to mass spectrometry, were applied to citratoperoxo precursor gels and films of $(\text{Bi,Nd})_4\text{Ti}_3\text{O}_{12}$ (BNdT). A slow heating rate resulted in secondary phases ($\text{Bi}_2\text{Ti}_2\text{O}_7$ and Bi_2O_3) while a high rate yielded phase pure layered perovskite BNdT. Comparison of the evolved gas profiles from the bulk gel and thin film, showed complete decomposition of the film at lower temperature than expected from thermogravimetric and evolved gas analysis of the bulk gel. Thermal methods adapted to thin films, therefore are crucial for understanding and controlling the oxide formation in the film.

Keywords Sol–gel · Thermal treatment · TG · In situ HT-XRD · FTIR · MS

Introduction

Neodymium substituted bismuth titanate $(\text{Bi,Nd})_4\text{Ti}_3\text{O}_{12}$, BNdT) is a layer-structured perovskite material, characterized by the so-called Aurivillius crystal phase [1]. The material shows interesting ferroelectric properties, such as a

relatively high remanent ferroelectric polarization, fatigue resistance on Pt substrates and a relatively low processing temperature in the order of 650 °C [2–4]. The fatigue resistance is engineered by the substitution of Bi^{3+} with lanthanide ions, and is explained by the non volatility of lanthanide oxide, as opposed to bismuth oxide, thus contributing to the reduction of the number of oxygen vacancies. This was first demonstrated for the case of La^{3+} and it inspired research efforts towards other lanthanides as well [5]. Another advantage of $(\text{Bi,Nd})_4\text{Ti}_3\text{O}_{12}$ is its lead-free composition. Together, these properties make it a candidate for commercial applications, e.g., for the production of non-volatile ferroelectric random access memories (FeRAM) or metal ferroelectric insulator semiconduction field effect transistors (MFIS-FET) [6].

In our laboratory, an entirely aqueous chemical synthesis route is researched for the preparation of metal oxide materials [7–11]. In this method, the metal ions are stabilized in an aqueous solution by complexation with chelating ligands such as peroxide and citrate. These homogeneous precursor solutions are stable in ambient conditions for extended periods of time. The optimized solutions can be evaporated and then transform to an amorphous, solid gel precursor or alternatively they can be applied for spin coating onto a suitable substrate in order to obtain thin films. To achieve a good wettability, the substrate needs to be subjected to a chemical pretreatment turning it hydrophilic [12]. After gelation or deposition, organic components are thermo-oxidatively removed by an optimized thermal treatment to yield the phase pure metal oxide. The route provides excellent composition control, due to the high degree of homogeneity, is inexpensive and allows uncomplicated deposition of films with a thickness ranging from several hundreds of nm down to a few nm [13] and even segregated islands [14].

A. Hardy (✉) · H. Van den Rul · M. K. Van Bael · J. Mullens
Institute for Materials Research, Laboratory of Inorganic and Physical Chemistry, Hasselt University, Diepenbeek, Belgium
e-mail: an.hardy@uhasselt.be

A. Hardy · H. Van den Rul · M. K. Van Bael
Division IMOMECE, IMEC vzw, Diepenbeek, Belgium

A. Hardy
Department of Applied Engineering Sciences, XIOS Hogeschool Limburg, Diepenbeek, Belgium

Here, we present a study of the formation of neodymium substituted bismuth titanate thin films from an aqueous solution–gel route, by using hyphenated thermal analysis, infrared spectroscopy and X-ray diffraction. The effectiveness of thermal methods for the purpose of studying oxide formation in films has been illustrated limitedly before [15–17], in contrast with the synthesis of powders where these methods are well established [18–21]. Here, we focus mainly on the differences between decomposition of bulk gels compared to thin films. The thermal methods applied here, play a pivotal role in understanding the different stages of the fabrication process of phase pure $(\text{Bi,Nd})_4\text{Ti}_3\text{O}_{12}$ films.

Experimental details

The synthesis of the precursor solution for the composition $\text{Bi}_{3.5}\text{Nd}_{0.5}\text{Ti}_4\text{O}_{12}$ was carried out entirely analogously to the route reported previously [22], except for replacing La^{3+} with Nd^{3+} . Commercial bismuth citrate ($\text{Bi}(\text{C}_6\text{H}_5\text{O}_7)_3$, 99.99%, Aldrich) is dissolved in water by addition of $\text{NH}_3(\text{aq})$ (32%, Merck, extra pure) and stabilized by monoethanolamine ($\text{C}_2\text{H}_7\text{NO}$ redistilled, 99.5+%, Aldrich). Neodymium citrate, synthesized from Nd_2O_3 (Alfa Aesar, 99.9%) and citric acid ($\text{C}_6\text{H}_8\text{O}_7$, 99%, Aldrich), is dissolved in water using ammonia and monoethanolamine. Citratoperoxo-Ti(IV) is synthesized by hydrolyzing Ti(IV)isopropoxide ($\text{Ti}(\text{iOPr})_4$, 98+%, Acros), in water, reacting the hydrolysis product with hydrogen peroxide (H_2O_2 , 35% wt in H_2O , p.a., stabilized, Acros) and citric acid and increasing pH with $\text{NH}_3(\text{aq})$. All the monometal ion solutions have a pH ~ 7 –7.5 and their exact concentration is verified using ICP-AES (Optima 3000, Perkin Elmer). They are combined in the desired ratio in order to obtain the stoichiometric multimetal ion precursor solution. The solution can be gelled upon evaporation in a furnace at 60 °C (24 h typically) or alternatively applied for spin-coating of thin films. The substrates used were Pt/BKB (best known barrier), chemically pretreated using a sulfuric acid–peroxide mixture, followed by an ammonia–hydrogen peroxide mixture, to render them hydrophilic. Depositions were carried out by spinning at 3,000 rpm during 30 s with a ramp of 1,000 rpm s^{-1} . Each layer was subjected to a stepwise thermal treatment on hot plates at increasing temperature in ambient air (160 °C—1 min, 260 °C—2 min, 480 °C—2 min). For the absorption–reflection Fourier transform infrared (AR-FTIR) study, the films were heat treated on hot plates up to the temperatures specified below. Finally, the films optionally are crystallized by rapid thermal processing in dry air up to a temperature of 650 °C (heating rate 50 °C s^{-1} , isothermal period 30 min).

In situ study of the phase formation in thin films was carried out using a modified Siemens D5000 (Cu K_α radiation). Here, the films were heated at a heating rate of 10 °C min^{-1} with an isothermal period of 130 min in order to collect the diffraction pattern with a sufficiently high signal to noise ratio. XRD patterns were collected at 376, 424, 472, 520, 570, 620, 670, and 721 °C. FTIR spectra are obtained using a Bruker IFS48 spectrometer, equipped with an absorption–reflection accessory for measurement of thin films (resolution 4 cm^{-1}). KBr pellets were prepared to study the solid gel powder. Thermogravimetric analysis was carried out using a TA Instruments TGA 951-2000. For evolved gas analysis, this was coupled on-line to a quadrupole mass spectrometer (Thermolab, VG Fisons).

Results and discussion

Generally, in wet chemical synthesis routes such as sol-gel, metalorganic decomposition, Pechini routes, etc. [23] the temperatures for the hot plate steps in film deposition are selected based on thermal analysis of a bulk gel or precursor powder. This approach is usually justified by the similarity of the chemical structure of a bulk precursor gel and the dried gel film, which are obtained by evaporation or chemical crosslinking of a precursor sol(ution), or by spin drying and subsequent heating steps, respectively.

Chemical structure of the precursor

The chemical structure of the $\text{Bi}_{3.5}\text{Nd}_{0.5}\text{Ti}_3\text{O}_{12}$ precursor gel, obtained by evaporation of an aqueous citratoperoxo precursor solution, was studied using FTIR (Fig. 1).

O–H, N–H, and C–H stretching vibrations are observed in the wavenumber region from 3,500 to 2,800 cm^{-1} .

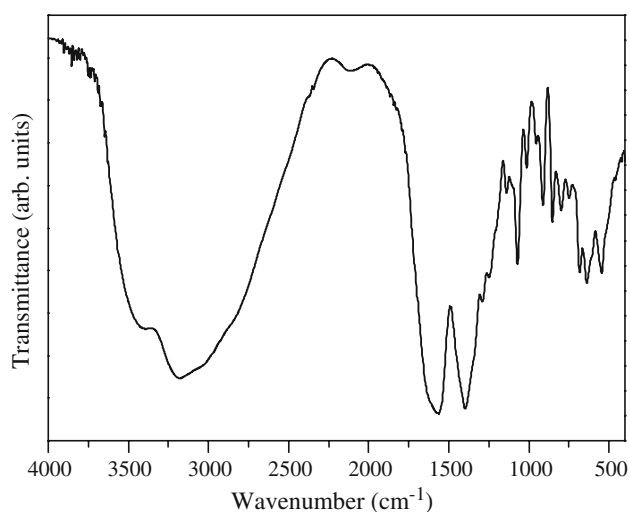


Fig. 1 FTIR spectrum of a BNdT precursor gel dried at 60 °C—24 h

Ammonium carboxylates are identified from their asymmetric and symmetric stretching vibrations at $1,580$ and $1,390\text{ cm}^{-1}$, respectively. Around $1,080\text{ cm}^{-1}$ a sharp C–O vibration is observed, which could be ascribed to the α -C–O(–H or –M) in citrato-ligands and ammonium citrate, possibly coordinating the metal ions. The chemical structure of citratoperoxo gels has been extensively studied in our research group, e.g., [7, 24]. It consists of metal ion complexes, surrounded by and bonded to a network formed of the excess ammonium citrate [25]. The ammonium ions allow the formation of hydrogen bridges between the excess citrate molecules and chelates, thereby ensuring the gel's amorphous and homogeneous nature.

The precursor gel's FTIR spectrum can be compared to the dried gel film, heat treated on a hot plate at $60\text{ }^\circ\text{C}$ in ambient air (Fig. 2). The similarity of the chemical structure in the film and the gel is clearly demonstrated. A vibration at $1,720\text{ cm}^{-1}$ which is present in the film but not in the gel, is indicative of –COOH groups, formed by NH_3 loss from –COONH₄. Furthermore, the vibration centered at $2,345\text{ cm}^{-1}$ are ascribed to artifacts from ambient CO₂.

Thermo-oxidative decomposition of the precursor

In Fig. 3 curves and derivative curves of the BNdT precursor gel are shown, measured at different heating rates. In accordance with previous experience, e.g., [25, 26] with the thermo-oxidative decomposition of citratoperoxo precursor gels for different metal oxides, in the case of BNdT the decomposition occurs in three distinct steps as well. The first step is ascribed to the decomposition of the excess of ammonium citrate, the second step to the decomposition of the chelating ligands and the third step to the removal of residual organic derivatives formed from the partially decomposed organic matrix. The selection of the hot plate

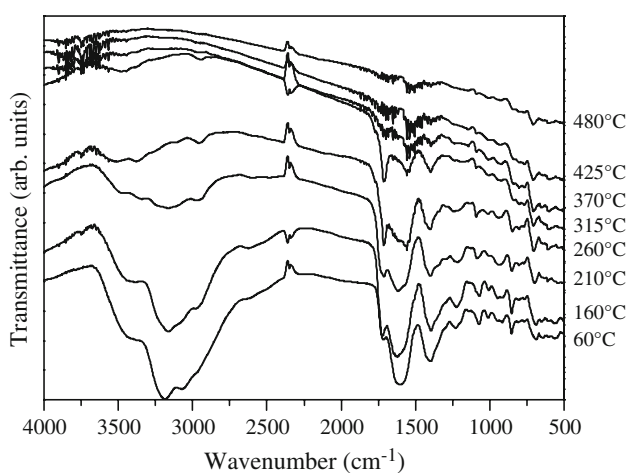


Fig. 2 Absorption–reflection FTIR spectra of BNdT films hot plate treated up to the indicated temperatures (ambient air)

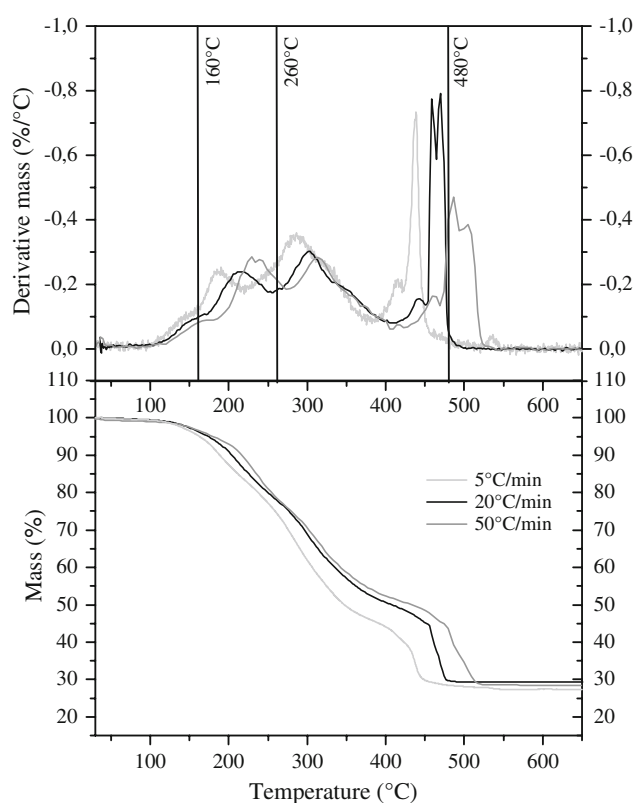


Fig. 3 Thermogravimetric analysis of BNdT precursor gel as a function of heating rate, illustration of the selected hot plate steps (100 mL min^{-1} dry air) in the derivative curve

treatment steps is illustrated in Fig. 3 as well. As expected, the individual decomposition steps shift towards higher temperature with increasing the heating rate from 5 to 20 to $50\text{ }^\circ\text{C min}^{-1}$, e.g., for the third step from $438\text{ }^\circ\text{C}$ to $465\text{ }^\circ\text{C}$ to $493\text{ }^\circ\text{C}$ (the reported temperature is at the maximum decomposition rate). A direct study of the BNdT film using TG was not feasible. First of all, the mass of a thin film (in the order of 100 nm final oxide thickness) is very small and changes due to thermal decomposition would be most difficult or impossible to detect. Furthermore, at high temperatures in oxidative environment, Si from the substrate would oxidize as well. This would lead to a mass increase, interfering with the mass decrease from the decomposition of the organic film components.

In order to still be able to study the thermo-oxidative decomposition of a thin BNdT film in a direct manner, here we applied evolved gas analysis by mass spectrometry. For the precursor gel, TG–MS measurements were carried out as normal, while for the films, the TG was simply applied as a furnace to heat the film. The sample was cut into pieces of the right size and placed inside the tube near the thermocouple. Mass spectra of the evolving gases were recorded without registering the mass changes (Fig. 4).

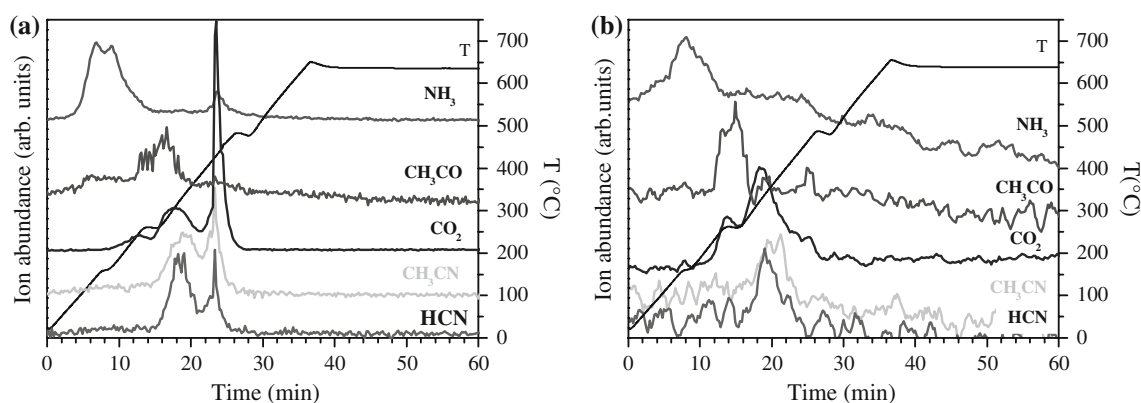


Fig. 4 Evolved gas analysis of dried **a** BNdT precursor gel, **b** BNdT precursor film showing the temperature profile and traces of $m/z = 17$ (NH_3), $m/z = 43$ (CH_3CO), $m/z = 44$ (CO_2), $m/z = 41$ (CH_3CN) and $m/z = 27$ (HCN) as a function of time (100 mL min^{-1} dry air, $20 \text{ }^\circ\text{C min}^{-1}$; isothermal periods simulating the stepwise film heat treatment temperatures of 160, 260, 480, and $650 \text{ }^\circ\text{C}$)

A detailed discussion of the typical decomposition of citratoperoxo precursor gels has been given in a previous paper, e.g., for the case of lanthanum substituted bismuth titanate [25]. The general decomposition scheme applies for the neodymium substituted bismuth titanate gel as well, due to the similarity of the precursors and lanthanide ions. Therefore, here we only focus on comparing the evolved gas analysis (EGA) of the BNdT bulk precursor gel to the thin film. The EGA results are also linked to the residual organics present in the solid phase, which were studied using AR-FTIR (Fig. 2). In the first decomposition step, NH_3 is evolved due to the decomposition reaction of $-\text{COONH}_4$ yielding $-\text{COOH}$ groups. This reaction is mainly occurring at a temperature around $160 \text{ }^\circ\text{C}$, for both the gel and the film. It can be linked to the increased intensity of the $-\text{COOH}$ vibration at $1,720 \text{ cm}^{-1}$ in AR-FTIR (Fig. 2) and changes in the spectral region around $3,250 \text{ cm}^{-1}$, after heat treatment of the film at $160 \text{ }^\circ\text{C}$. At the same time, a competitive dehydration of ammonium carboxylate leads to the formation of amides, but the amide I and II bands are overlapping with the remaining carboxylates and carboxylic acids. The onset of decomposition of these $-\text{COOH}$ groups by decarboxylation, is observed at slightly higher temperatures, as is indicated by the first evolution of CO_2 around $260 \text{ }^\circ\text{C}$ for both the gel and the film. Furthermore, decomposition products of citric acid, indicated by CH_3CO ($m/z 43$), are observed in this temperature region for both samples as well, extending up to slightly higher temperatures for the gel. In the solid phase, the AR-FTIR spectra after heat treatment at 210 and $260 \text{ }^\circ\text{C}$ support the conclusions concerning the decomposition of the carboxylate and formation of nitrogen containing organic derivatives, which were based on the EGA. A decrease of the O–H, N–H, and C–H bands in the $3,500\text{--}3,000 \text{ cm}^{-1}$ region is evident. Changes are observed in the carboxylate region such as decreasing intensity and peak shifts caused by the formation of decomposition products of the ammonium

carboxylates and complexes. During the temperature increase between 260 and $480 \text{ }^\circ\text{C}$, the evolution of CO_2 intensifies and N-containing decomposition products such as CH_3CN and HCN are observed for both the gel and the film. When $480 \text{ }^\circ\text{C}$ is reached, in the case of the film the evolution of volatile organic decomposition products is nearly ended, with only a small amount of CO_2 and possibly also still some CH_3CO being observed. The AR-FTIR spectra show virtually no organic components from $370 \text{ }^\circ\text{C}$ onwards (note an artifact due to ambient H_2O vapor in the broad region around $1,500 \text{ cm}^{-1}$). This is a contrast with the bulk gel, where organics are still decomposing up to around $450 \text{ }^\circ\text{C}$ at the same heating profile, which leads to the evolution of the largest amounts of CO_2 , CH_3CN and HCN . This difference between the bulk gel and film is ascribed to the different surface to volume ratio, which leads to a more efficient decomposition product removal in the film. Possibly, the formation of thermostable nitrogen containing organic derivatives in the film subsequently could be less pronounced than in the bulk gel. To these differences, the film's lower apparent decomposition temperature could be ascribed.

In conclusion, by comparison of the bulk and thin film decomposition behavior using evolved gas analysis and absorption–reflection FTIR, it becomes clear that important differences can exist. This has interesting implications for the selection of the heat treatment of the film.

Oxide phase formation

The in situ HT-XRD measurement (Fig. 5a) showed that the BNdT film remained amorphous up to $424 \text{ }^\circ\text{C}$, while the formation of the crystalline BNdT Aurivillius phase (JCPDS card 35-0795) is observed from $472 \text{ }^\circ\text{C}$ onwards. This crystallization is seen to immediately follow up on the temperature at which the CO_2 volatilization from the film ended according to evolved gas analysis. However, a

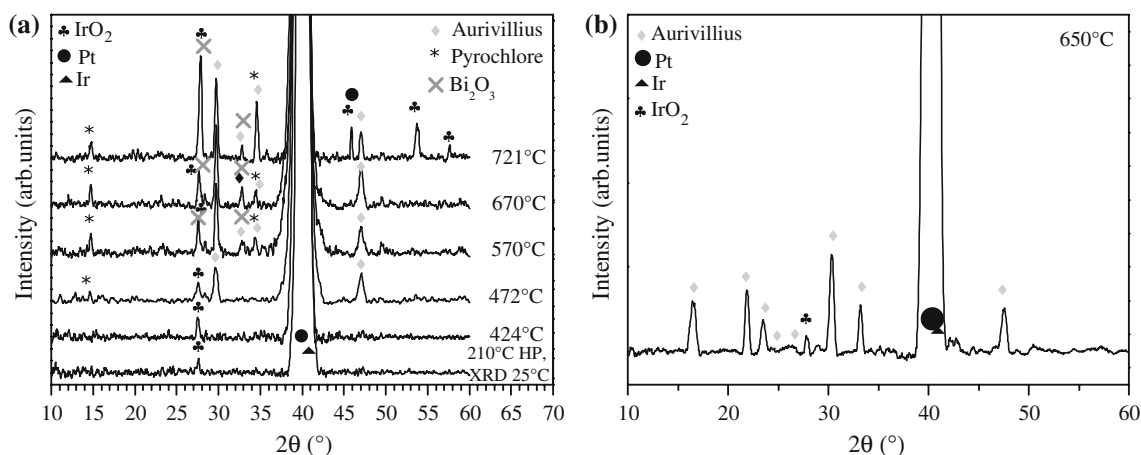


Fig. 5 Crystalline phase formation of the BNdT film **a** in situ HT-XRD in static air, **b** room temperature XRD after RTP up to 650 °C in dynamic dry air

secondary pyrochlore phase, of the composition $\text{Bi}_2\text{Ti}_2\text{O}_7$, is observed as well. This parasitic phase remains present up to the high temperature of 721 °C, where the substrate structure is destabilized as evidenced by the increased intensity of IrO_2 adhesion layer peaks. Furthermore, starting from 570 °C a secondary bismuth oxide phase is observed from the growing intensity of its diffraction peak at $27.6^\circ 2\theta$, which also remains up to high temperature. Though IrO_2 from the substrate also shows a diffraction peak around this position, other IrO_2 peaks at $53.7^\circ 2\theta$ and $57.7^\circ 2\theta$ are not observed until 721 °C. This indicates that it is rather Bi_2O_3 , which is formed at 570 °C. In contrast with the HT-XRD measurement, after hot plate treatment as described in the experimental section and rapid thermal processing of a film up to 650 °C, a phase pure Aurivillius oxide is obtained in the BNdT film (Fig. 5b). The difference in both results is ascribed to the strong difference in heating rate. While the RTP treatment heats the BNdT film up to 650 °C in 2 min and 3 seconds (2 min up to 500 °C, 50°C s^{-1} from 500 to 650 °C), the HT-XRD measurements were carried out in a much longer time span (1,111 min) due to the requirement of obtaining a sufficient signal to noise ratio. The kinetics of the oxide formation affect the nucleation phenomena, determining the formation of a phase pure BNdT thin film. A fast heating rate is sufficient to avoid nucleation of secondary phases, based on a comparison of Fig. 5a and b.

Conclusion

The formation mechanism of BNdT in thin films on platinumized silicon was studied by applying thermal methods, specifically adapted to coatings.

Crystalline phase formation was studied using in situ HT-XRD and off-line XRD, which demonstrated that Aurivillius phase BNdT can crystallize in the film at a temperature as low as $\sim 470^\circ\text{C}$. Though phase pure films were obtained after RTP treatment, in HT-XRD secondary phase formation was observed. The latter was ascribed to the much slower heating profile leading to different nucleation phenomena. Therefore, HT-XRD with the current technical setup can only be applied to estimate a possible minimum temperature for oxide crystallization, but conclusions concerning phase purity should be drawn with due care.

The thermal decomposition leads to chemical structural changes in the solid phase of the films, and to gas evolution. These were studied by absorption-reflection FTIR and by evolved gas analysis through MS. A comparison with TG-MS of a bulk BNdT gel precursor showed that the thermo-oxidative decomposition of the thin films is more efficient than that of bulk powders. As a consequence, starting from 370 °C, virtually no more organics are observed in the FTIR spectra of thin BNdT films, while the evolved gas analysis of the bulk powder indicated that at least 450 °C is needed (heating rate $20^\circ\text{C}/\text{min}$ with intermediate isothermal steps). Therefore, we conclude that using TG and evolved gas analysis of a bulk precursor, to select a heat treatment scheme for thin films can lead to overestimation of the actual required temperatures. Thin film evolved gas analysis in combination with AR-FTIR study of the chemical structural evolution in the solid phase, may provide a more solid base for this.

Acknowledgments A. Hardy and M. K. Van Bael are postdoctoral research fellows of the Research Foundation Flanders (FWO-Vlaanderen). Dr. G. Vanhoyland is gratefully acknowledged for carrying out the X-ray diffraction measurements and the authors thank Dr. Ir. D. J. Wouters at IMEC-Leuven for supplying the platinumized silicon substrates.

References

- Aurivillius B. Mixed bismuth oxides with layer lattices II. Structure of $\text{Bi}_4\text{Ti}_3\text{O}_{12}$. *Ark Kemi*. 1949;1:499–512.
- Hou F, Shen MR, Cao WW. Ferroelectric properties of neodymium-doped $\text{Bi}_4\text{Ti}_3\text{O}_{12}$ thin films crystallized in different environments. *Thin Solid Films*. 2005;471:35–9.
- Kojima T, Sakai T, Watanabe T, Funakubo H, Saito K, Osada M. Large remanent polarization of $(\text{Bi,Nd})_4\text{Ti}_3\text{O}_{12}$ epitaxial thin films grown by metalorganic chemical vapor deposition. *Appl Phys Lett*. 2002;80:2746–8.
- Gao XS, Xue JM, Wang J. Ferroelectric behaviors and charge carriers in Nd-doped $\text{Bi}_4\text{Ti}_3\text{O}_{12}$ thin films. *J Appl Phys*. 2005;97:034101.
- Park BH, Kang BS, Bu SD, Noh TW, Lee J, Jo W. Lanthanum-substituted bismuth titanate for use in non-volatile memories. *Nature*. 1999;401:682–4.
- Zang YY, Xie D, Xiao YH, Ruan Y, Ren TL, Liu LT. Interface studies and electronic properties of silicon based Nd-doped bismuth titanate. *Integr Ferroelectr*. 2008;98:90–6.
- Hardy A, D'Haen J, Van Bael MK, Mullens J. An aqueous solution-gel citratoperoxo-Ti(IV) precursor: synthesis, gelation, thermo-oxidative decomposition and oxide crystallization. *J Sol–Gel Sci Technol*. 2007;44:65–74.
- Hardy A, D'Haen J, Goux L, Wouters DJ, Van Bael M, Van den Rul H, et al. Aqueous chemical solution deposition of ferroelectric Ti^{4+} cosubstituted $(\text{Bi,Ln})_4\text{Ti}_3\text{O}_{12}$ thin films. *Chem Mater*. 2007;19:2994–3001.
- Van Werde K, Vanhoyland G, Mondelaers D, Van den Rul H, Van Bael M, Mullens J, et al. The aqueous solution-gel synthesis of perovskite $\text{Pb}(\text{Zr}_{1-x}\text{Ti}_x)\text{O}_3$ (PZT). *J Mater Sci*. 2007;42:624–32.
- Pagnaer J, Hardy A, Mondelaers D, Vanhoyland G, D'Haen J, Van Bael MK, et al. Preparation of $\text{La}_{0.5}\text{Sr}_{0.5}\text{CoO}_3$ powders and thin film from a new aqueous solution-gel precursor. *Mater Sci Eng B Solid State Mater Adv Technol*. 2005;118:79–83.
- Nelis D, Mondelaers D, Vanhoyland G, Hardy A, Van Werde K, Van den Rul H, et al. Synthesis of strontium bismuth niobate ($\text{SrBi}_2\text{Nb}_2\text{O}_9$) using an aqueous acetate-citrate precursor gel: thermal decomposition and phase formation. *Thermochim Acta*. 2005;426:39–48.
- Van Bael MK, Nelis D, Hardy A, Mondelaers D, Van Werde K, D'Haen J, et al. Aqueous chemical solution deposition of ferroelectric thin films. *Integr Ferroelectr*. 2002;45:113–22.
- Hardy A, Van Elshocht S, Adelman C, Conard T, Franquet A, Douhéret O, et al. Aqueous solution-gel preparation of ultrathin ZrO_2 films for gate dielectric application. *Thin Solid Films*. 2008;516:8343–51.
- De Dobbelaere C, Hardy A, D'Haen J, Van den Rul H, Van Bael MK, Mullens J. Morphology of water-based chemical solution deposition (CSD) lead titanate films on different substrates: towards island formation. *J Eur Ceram Soc*. in press 2008.
- Horvath E, Kristof J, Vazquez-Gomez L, Redey A, Vagvolgyi V. Investigation of $\text{RuO}_2\text{-IrO}_2\text{-SnO}_2$ thin film evolution - A thermoanalytical and spectroscopic study. *J Therm Anal Calorim*. 2006;86:141–6.
- Horvath E, Kristof J, Frost RL, Heider N, Vagvolgyi V. Investigation of $\text{IrO}_2/\text{SnO}_2$ thin film evolution by thermoanalytical and spectroscopic methods. *J Therm Anal Calorim*. 2004;78:687–95.
- Wang MH, Tokiwa S, Nishide T, Kasahara Y, Seki S, Uchida T, et al. Thermally induced changes in amorphous indium-tin-oxide thin films. *J Therm Anal Calorim*. 2008;91:249–54.
- Du XF, Xu YL, Ma HX, Wang J, Li XF. Low-temperature synthesis of bismuth titanate by an aqueous sol-gel method. *J Am Ceram Soc*. 2008;91:2079–82.
- Thongtem T, Thongtem S. Characterization of $\text{Bi}_4\text{Ti}_3\text{O}_{12}$ powder prepared by the citrate and oxalate coprecipitation processes. *Ceram Int*. 2004;30:1463–70.
- Zaremba T. Investigation of synthesis and microstructure of bismuth titanates with TiO_2 rich compositions. *J Therm Anal Calorim*. 2008;93:829–32.
- Prakash P, Garg A, Roy MK, Verma HC. Novel low-temperature synthesis of ferroelectric neodymium-doped bismuth titanate nanoparticles. *J Am Ceram Soc*. 2007;90:1295–8.
- Hardy A, Nelis D, Vanhoyland G, van Bael MK, Mullens J, van Poucke LC, et al. Aqueous CSD of ferroelectric $\text{Bi}_{3.5}\text{La}_{0.5}\text{Ti}_3\text{O}_{12}$ (BLT) thin films. *Integr Ferroelectr*. 2004;62:205–9.
- Schwartz RW, Schneller T, Waser R. Chemical solution deposition of electronic oxide films. *CR Chim*. 2004;7:433–61.
- Van Werde K, Vanhoyland G, Nelis D, Mondelaers D, Van Bael MK, Mullens J, et al. Phase formation of ferroelectric perovskite $0.75\text{Pb}(\text{Zn}_{1/3}\text{Nb}_{2/3})\text{O}_3\text{-}0.25\text{BaTiO}_3$ prepared by aqueous solution-gel chemistry. *J Mater Chem*. 2001;11:1192–7.
- Hardy A, Vanhoyland G, Geuzens E, Van Bael MK, Mullens J, Van Poucke LC, et al. Gel structure, gel decomposition and phase formation mechanisms in the aqueous solution-gel route to lanthanum substituted bismuth titanate. *J Sol–Gel Sci Technol*. 2005;33:283–98.
- Truijen I, Hardy A, Van Bael MK, Van den Rul H, Mullens J. Study of the decomposition of aqueous citratoperoxo-Ti(IV)-gel precursors for titania by means of TGA-MS and FTIR. *Thermochim Acta*. 2007;456:38–47.